Hindawi
International Journal of Polymer Science
Volume 2018, Article ID 7842148, 12 pages
https://doi.org/10.1155/2018/7842148

Research Article

Graphene Oxide-PES-Based Mixed Matrix Membranes for Controllable Antibacterial Activity against *Salmonella typhi* and Water Treatment

Haleema Tariq Bhatti,[1] Nasir M. Ahmad,[1] Muhammad Bilal Khan Niazi,[2] Muhammad Azeem Ur Rehman Alvi,[1] Naveed Ahmad,[3] Muhammad Nabeel Anwar,[4] Waqas Cheema,[2] Sheraz Tariq,[1] Mehwish Batool,[5] Zaeem Aman,[2] Hussnain A. Janjua,[6] Asim Laeeq Khan,[5] and Asad U. Khan[5]

[1]*Polymer Research Lab, Department of Materials Engineering, School of Chemical & Materials Engineering (SCME), National University of Sciences and Technology, Islamabad, Pakistan*
[2]*Department of Chemical Engineering, School of Chemical and Materials Engineering, National University of Sciences and Technology, Islamabad, Pakistan*
[3]*Department of Pharmacy, Quaid-i-Azam University, Islamabad, Pakistan*
[4]*Department of Biomedical Engineering and Sciences, School of Mechanical & Manufacturing Engineering (SMME), National University of Sciences and Technology, Islamabad, Pakistan*
[5]*Department of Chemical Engineering, COMSATS Institute of Information Technology, Lahore, Pakistan*
[6]*Department of Industrial Biotechnology, Atta-ur-Rahman School of Applied Biosciences (ASAB), National University of Sciences and Technology, Islamabad, Pakistan*

Correspondence should be addressed to Nasir M. Ahmad; nasir.ahmad@scme.nust.edu.pk

Received 22 May 2018; Revised 16 August 2018; Accepted 29 August 2018; Published 18 November 2018

Academic Editor: Hossein Roghani-Mamaqani

The present work is focused on preparation, characterization, and antibacterial activity evaluation of graphene oxide/polyethersulfone mixed matrix filtration membranes. Graphene oxide (GO) was synthesized via improved Hummer's method and characterized by XRD, FTIR, and SEM. FT-IR spectra showed the presence of carboxylic acid and hydroxyl groups on GO nanosheets. Different concentrations of the synthesized GO at 0.25, 0.5, and 1.0 wt. % were incorporated in polyethersulfone (PES) matrix via phase inversion method to fabricate GO-PES membranes. Increasing porosity and formation of wider, finger-like channels were observed with increased GO concentrations relative to pristine membranes as evident from scanning electron microscopy (SEM) micrographs of the fabricated membranes. However, membranes prepared with 1 wt. % GO appear to contain aggregation and narrowing of pore morphology. GO-incorporated membranes demonstrated enhanced flux, water-retaining capacities, and wettability as compared to pristine PES membranes. Shake flask and colony counting methods were employed to carry out antibacterial testing of synthesized GO and fabricated GO-PES membranes against *Salmonella typhi* (*S. typhi*)—a gram-negative bacteria present in water that is known as causative agent of typhoid. Synthesized GO showed significant reduction up to 70.8% in *S. typhi* cell count. In the case of fabricated membranes, variable concentrations of GO are observed to significantly influence the percentage viability of *S. typhi*, with reduction percentages observed at 41, 60, and 69% for 0.25, 0.5, and 1.0 wt. % GO-incorporated membranes relative to 17% in the case of pristine PES membranes. The results indicate a good potential for applying GO/PES composite membranes for water filtration application.

1. Introduction

More than 1 billion people on earth are deprived of the basic human need that is access to potable water [1]. As reported by the World Health Organization (WHO), in the year 2017, around 2.5 billion people around the globe were devoid of adequate sanitation, in addition to hundreds of millions having no access to water at all [2]. It is important to mention that even though two-thirds of the Earth's surface is covered with water, however, fresh water sources make up a mere 2.5% of the global water distribution [3]. Furthermore, our limited water resources are being polluted with passing time and the accumulation of waste and pollutants in water is making water unsafe for human use [4]. In addition to depleting fresh water sources and deteriorating water quality due to poor water management, booming global population, increasing urbanization, industrialization, and expanding economies are further increasing the global water demand [5]. Waterborne diseases (e.g., hepatitis (A, E), typhoid, and cholera) are a major factor of morbidity and mortality in developing countries, and millions of lives are lost every year due to use of untreated water [6, 7]. For example, typhoid fever is known as a major public health concern that is caused by a gram-negative bacterium *Salmonella enterica* serotype typhi (*S. typhi*). It is a leading cause of mortality and morbidity in developing countries, especially in Asia [8]. Around 24.2 million cases of typhoid fever with around 75,000–208,000 deaths were reported during 2016 [9].

In consideration of the abovementioned reports, presently, there are extensive research efforts being undertaken to improve healthy water supply that is free from contamination, especially free from bacteria [10–12]. In this context, owing to their efficiency, modular design, low-energy requirement, and environment friendly-working with minimal use of chemicals, membrane technology has been dramatically increasing its share in the market of water treatment technologies over the past few years [13]. Despite having an array of advantages over other traditional water treatment modalities and the ability to perform various functions, membrane technology has its own set of drawbacks when it comes to water treatment: fouling, decline in flux overtime, hydrophobicity of polymers used, etc. [14]. Also, depending on processing conditions and composition of the solution, filtration of microscopic particles (such as bacteria and viruses) may not be completed. Therefore, development of high-performance membranes to overcome these setbacks and/or improve performance is an active field of research since the past several decades and nanotechnology is playing a major role in it [13, 15–17]. Advances in membrane materials and modification and development of currently existing membranes can be employed to make membranes with enhanced efficiency and performance [18–22].

Furthermore, the role of polymer matrix itself is highly significant to prepare membranes with desirable mechanical, morphological, and surface properties. Thus, certain polymers are widely employed to fabricate membranes [21]. For example, polyethersulfone (PES) is among the commonly used polymers for fabrication of water filtration membranes [23] as it possesses numerous beneficial properties including excellent mechanical properties, high-dimensional stability, thermal stability, remarkable oxidative and hydrolytic stability, mechanical robustness, and tolerance to solvents [24]. However, despite these remarkable characteristics, PES is hydrophobic in nature and requires preferably containing certain degrees of hydrophilic character to exhibit higher flux. This can be achievable through incorporation of functional groups and materials [23–28]. Among various approaches, incorporation of graphene oxide (GO) appears to be highly attractive for multiple purposes owing to enhance surface wettability as well as antibacterial activity [29–38]. Currently, significant research efforts are underway to investigate the effect of GO against bacterial detection and control contamination in water to treat it. For example, filtration membranes composed of PES and graphene oxide were investigated for membrane bioreactors for dairy wastewater treatment [39, 40]. In another work, graphene oxide is modified with polyethyleneimine and then mixed with PES casting solution to develop antibacterial activity against *E. coli* [41]. In consideration of the wide range of bacterial contamination, there is a continuous need to carry out further research to overcome serious challenges of bacterial water contamination. For example, to the best of our knowledge, there are limited research works involving GO polymer membrane employment to treat *Salmonella typhi* bacteria, which is regarded as the leading cause of deaths in developing countries and results in infections causing diarrhoea [42]. Most of the work is related to treatment using ciprofloxacin and other related fluorinated 4-quinolones. These have pharmacokinetic and microbiological characteristics as effective agents in the treatment of typhoid fever. Against Salmonella typhi, ciprofloxacin has found to be as effective as chloramphenicol or cotrimoxazole. In addition, ciprofloxacin seems to eliminate chronic carriage of *S. typhi* as compared to other antibiotics [43–47]. In other related studies, nanocomposites of chitosan were employed as electrochemical DNA biosensors to detect typhoid due to Salmonella typhi. Probe on GO-CHI/ITO via glutaraldehyde was prepared through covalent immobilization of *S. typhi*-specific 5′-amine by labelling as single-stranded (ss) DNA. Studies indicated the capability of the developed sensor to distinguish various sequences. Performance was attributed to good electrochemical activity of graphene oxide and good biocompatibility of chitosan that increased DNA immobilization to facilitate the electron transfer process between the electrode surface and DNA [48].

In consideration of the abovementioned challenges, the present study was aimed at fabricating novel polyethersulfone membranes that exhibit controllable antibacterial effect against S. typhi due to incorporation of variable concentrations of graphene oxide for water treatment applications. To the best of our knowledge, GO polymer membranes have not been explored in detail by incorporating variable concentrations of GO to cover a broad range of antibacterial activity to overcome serious challenges associated with water contamination associated with the presence of S. typhi in it. Thorough characterization of the fabricated membranes including water flux, water retention, surface wettability, and percentage reduction of *S. typhi* colonies following

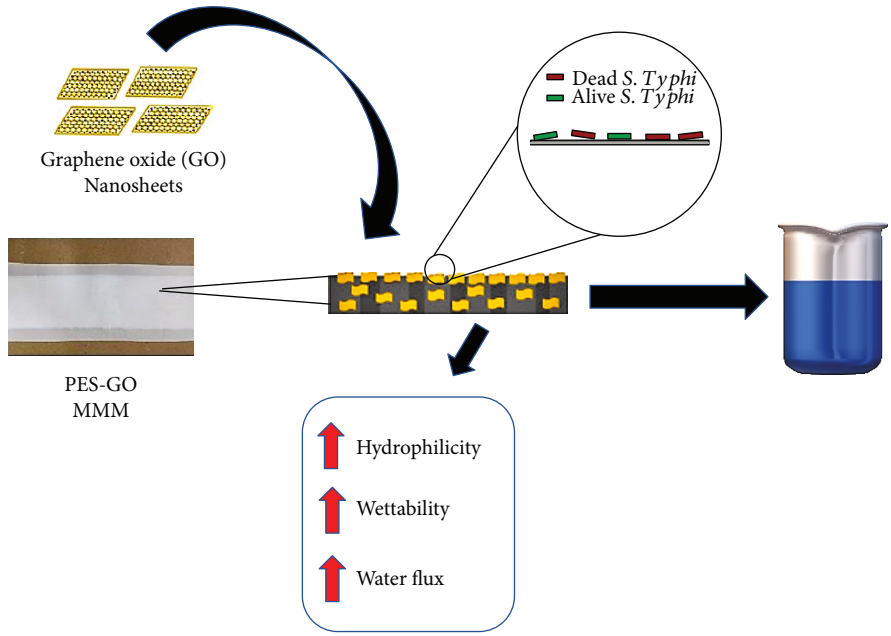

Figure 1: Graphical abstract.

interaction with various concentrations of GO in PES membranes has been discussed to highlight the importance of the fabricated membranes for water treatment.

2. Materials and Methods

2.1. Materials. Analytical grade chemicals were used throughout the experimental work and used as received unless specified. Polyethersulfone (PES) was obtained from Ultrasone, Germany. Graphite flakes, sulfuric acid (H_2SO_4, 95–98%), phosphoric acid (H_3PO_4, ≥85%), hydrochloric acid (HCl) (36%), potassium permanganate ($KMnO_4$), and N-methyl-2-pyrrolidione (NMP) were purchased from Sigma-Aldrich, Germany. Hydrogen peroxide (H_2O_2, 35%) was acquired from Merck, Germany. Nutrient agar was acquired from Thermo Fisher Scientific. *Salmonella typhi* (ATCC 6539) used for antibacterial testing was obtained from School of Mechanical and Manufacturing Engineering (SMME), National University of Sciences and Technology (NUST).

2.2. Synthesis of Graphene Oxide (GO). Improved Hummer's method was used to prepare large-area graphene oxide from graphite flakes. This method was chosen owing to its simplicity and efficiency in yielding large-area graphene oxide [49]. Synthesis of graphene oxide was carried out at room temperature by adding graphite flakes (2 g) to a stirring mixture of H_2SO_4 : H_3PO_4 (240 : 60 ml) in a pot, followed by the gradual addition of $KMnO_4$ (12 g). This dark purplish mixture of graphite flakes and oxidizing agents was kept on continuous stirring for 3 days, resulting in a colour change to dark brownish. H_2O_2 (~12 ml) was added in this brownish mixture to quench the process of oxidation, changing the colour of mixture from dark brown to mustard. The mixture, now graphite oxide, was then washed once with 1 M HCl. Subsequently, a thick graphene oxide gel-like solution was attained when the acid-washed pellet was centrifuged at 4000 rpm several times with distilled water until the pellet of the solution had achieved pH 6. This gel-like solution was vacuum dried at ~50°C to obtain graphene oxide.

2.3. Fabrication of PES-GO-Incorporated Mixed Matrix Membranes. Polymeric mixed matrix membranes were fabricated with variable concentrations of graphene oxide (GO) used as nanofiller in the PES polymer matrix and supported on polyester sheet. Figure 1 represents the graphical abstract of PES-GO mixed matrix membrane. Compositions of the prepared membranes are given in Table 1. Phase inversion based on immersion precipitation technique was used to fabricate the membranes. Magnetic stirring was carried out overnight at room temperature until the polymer was completely dissolved followed by casting of the solution to make the membranes. Pristine M1 PES membrane was prepared without any incorporation of GO. For the fabrication of graphene oxide-incorporated mixed matrix membranes, GO was added in three different concentrations (*w*/*w*): 0.25 wt. % as M2 membrane, 0.5 wt. % as M3, and 1 wt. % as M4 in NMP solvent and dissolved through magnetic stirring. The polyester support was wetted with solvent before membrane casting to prevent the polymer solution to penetrate the support. After spreading and casting the membranes with casting solution, the membranes were then immersed in coagulation bath (distilled water) for 10 min at room temperature. In the final step, membranes were dried under ambient conditions and were then stored for later use.

2.4. Characterization of GO and GO-PES Membranes. X-ray diffraction STOE θ was used to investigate the crystal structure of graphene oxide. The XRD analysis was performed for 2θ range from 5° to 55°. The XRD pattern was further

Table 1: GO concentration employed and composition of the prepared mixed matrix PES membranes with variable incorporated GO concentrations, water retention content, average contact angle, flux, and reduction of S. typhi cell values for the fabricated membranes and GO concentration employed.

GO concentrations (g)	Membrane type	Membrane composition	Water retention (%)	Average contact angle (°)	Flux ($l/m^2 \cdot h$)	Reduction of *S. typhi* cell membrane GO (%)	(%)
GO1 (0.00125)	M1	PES	32.71	68	27.94	17.30	27.80
GO2 (0.0025)	M2	PES + 0.25% GO	44.90	61°	50.00	41.00	48.00
GO3 (0.00625)	M3	PES + 0.50% GO	57.19	53°	142.10	60.10	57.10
GO4 (0.0125)	M4	PES + 1.00% GO	53.40	56°	41.26	69.40	70.80

analysed and compared with the literature. Fourier transform infrared spectroscopy was performed on in transmittance mode on Spectrum 100 (PerkinElmer) FTIR spectrometer. Graphene oxide dispersed and hydraulic pressed along KBr powder in a pellet form was used to characterize the functional groups of the sample. The scan of spectrum ranged from 450 cm^{-1} to 4000 cm^{-1}. The morphology of graphene oxide was analysed using SEM Joel JSM 6490A. Graphene oxide was sonicated in distilled water for 2-3 hours; a drop was poured on a steel stud and the sample was analysed following gold coating.

2.5. Water Retention Test and Permeate Flux. Water retention of the fabricated membranes was investigated by soaking 0.1 g of each membrane in distilled water for 24 hours, and wet weight was calculated. The membranes were then oven dried for 12 hours, and dry weight was calculated. The water retention capacity was calculated using the following relation [50].

$$\text{Water retention capacity} = \frac{(\text{wet weight} - \text{dry weight})}{\text{wet weight}} \times 100. \quad (1)$$

Permeation flux that is the volume of liquid water passing through the membrane per unit area per unit time of the fabricated membranes was calculated for pure water (distilled water). The test was performed using a custom-made vacuum filtrate assembly. Distilled water was passed through 0.025 m^2 of each membrane at a constant pressure of 79.99 KPa, and the time taken for the water to flow through the membranes was recorded. Permeation flux for pure water for each membrane was calculated using the following relation [51].

$$J = \frac{Q}{(A \times t)}, \quad (2)$$

where J is the permeate flux ($L \cdot m^{-2} \cdot h^{-1}$), Q is the volume of permeate/water passed through the membrane (in litres), A is the area of the membrane (m^2), and t is the time taken for filtration (in hours). Experimental error was minimized by taking at least five measurements for each membrane type.

2.6. Antibacterial Testing of GO and GO-PES Membranes against Salmonella typhi. Antibacterial activity of GO was assessed specifically against gram-negative bacterium—-*Salmonella typhi* (ATCC 6539)—through shake flask and colony counting method. *S. typhi* cells from a freshly prepared culture were used. The bacterial cells were cultured overnight at 37°C in nutrient broth. To test the antibacterial activity, GO with variable concentrations at 0 g, 0.00125 g, 0.0025 g, 0.00625 g, and 0.0125 g, designated as GO1, GO2, GO3, and GO4, respectively, was added into flasks containing 25 ml of sterile 0.9% saline and sonicated for 30 minutes. Subsequently, each flask was inoculated with 500 μl of bacterial suspension of *S. typhi* (diluted to $1–5 \times 10^7$ CFU/ml in the flask). Following inoculation, the flasks were incubated for 2 hours at 37°C on a rotary shaker for continuous gentle stirring of the contents. 1 ml was drawn from each flask at time intervals of 0 and 2 hours and spread on nutrient agar plates in triplicates. The plates were incubated overnight at 37°C, following which colonies on each plate were counted on a colony counter machine [52]. The percentage reduction of viable *S. typhi* counts was calculated using the following relation.

$$\%\ \text{reduction of S.Typhi counts} = \left(\frac{\text{no. of colonies at } T_0 - \text{no. of colonies at } T_t}{\text{no. of colonies at } T_0}\right) \times 100, \quad (3)$$

where T_0 is time at 0 hours and T_t is time at t hour. Percentage reduction was calculated for each plate from the triplicates, and an average was calculated.

Antibacterial activity of the fabricated GO-PES membranes was also tested against gram-negative bacterium—-*Salmonella typhi* (ATCC 6539)—through shake flask and colony counting methods. The bacterial cells were cultured overnight at 37°C in nutrient broth and used subsequently. All the materials used in this experiment were sterilized before use. To test the antibacterial activity of the fabricated membranes, each membrane type was cut in square having an area of 2.5 cm × 2.5 cm, following which they were immersed in flasks containing 100 ml sterile 0.9% saline. Each flask was inoculated with 500 μl of bacterial suspension of *S. typhi* (diluted to $1–5 \times 10^7$ CFU/ml in the flask). Following inoculation, the flasks were incubated for 8 hours at 37°C on a rotary shaker for continuous gentle stirring of the contents. 1 ml liquid was drawn from each flask at time intervals of 0 and 8 hours and spread on nutrient agar plates in triplicates. The plates were incubated overnight at 37°C following which colonies on each plate were counted on a colony counter machine. The percentage reduction of viable *S. typhi* counts following interactions with fabricated membranes for 8 hours was calculated using the relation given in (3). Following the shake flask method, the membranes were washed with saline and SEM was performed to visualize the bacteria on the membrane surface. Obtained results for GO and fabricated membranes were statistically analysed via unpaired *t*-test (two tailed) in "GraphPad Prism" software. A P value of ≤0.05 was considered significant.

3. Results and Discussion

3.1. Characterization of GO. The X-ray diffraction pattern is given in Figure 2, which showed an intense peak at an angle 2θ for graphene oxide. The smaller angle suggests greater interplanar distance among the GO sheets [53]. The peak at around 18-19 indicates the presence of graphite oxide in the sample.

Figure 3 shows the FTIR spectra of GO. The sharp peak at 3431 cm^{-1} corresponds to hydroxyl (O–H) stretching vibrations [54], while sharp peaks at 1622 cm^{-1} and 1417 cm^{-1} can be correlated to vibrations of skeletal aromatic rings—result of C=C stretching of the phenol rings. The peak at around 2921 cm^{-1} can be attributed to sp3/sp2 stretches. Peaks of

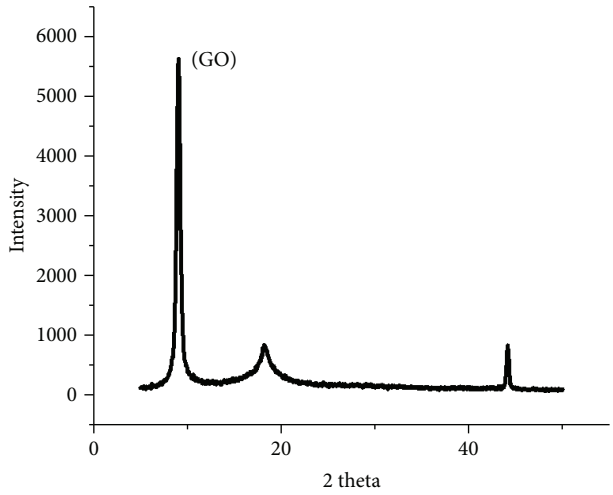

Figure 2: XRD pattern of the prepared graphene oxide (GO).

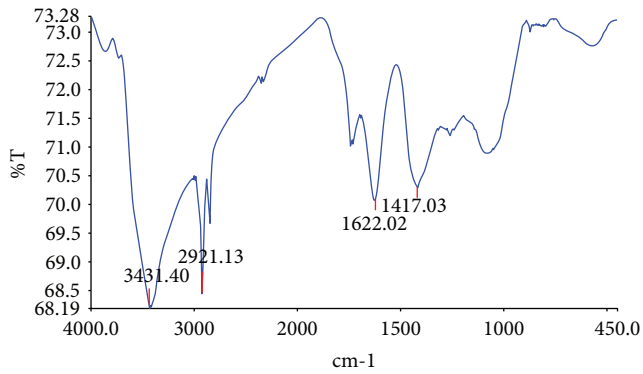

Figure 3: FTIR spectra of the prepared graphene oxide (GO).

carbonyl (C=O) stretching vibrations of the carboxylic group and hydroxyl (C-OH) groups can be seen at 1720 cm^{-1} and around 1243 cm^{-1} [54], respectively. A band of peak from around 1000 cm^{-1} to 1100 cm^{-1} can be related to the deformation of C-O bonds. SEM micrographs of GO showed the presence of exfoliated layers. These sheets of GO were transparent and wrinkled as shown in Figure 4.This indicates that GO sheets were exfoliated and single layered or multilayered sheets of GO were present in nanoscale [55].

3.2. Characterization of GO-PES Membranes

3.2.1. Morphological Structure and Porosity. Scanning electron micrographs which are given in Figure 5 show the change in porosity of membranes with different concentrations of GO incorporation. An increase in number of pores with the increasing GO concentration is observed. As seen in Figure 5, agglomeration and blockage of pores can be observed in M4 (membrane with 1 wt. % GO concentration); this can be attributed to the high concentration of GO [56]. Figure 6 also shows SEM micrographs of the fabricated membranes. Asymmetric structured membranes with a dense top layer and macrovoids in the lower region were observed. M1 pristine PES membrane with 0% GO concentration had the characteristic asymmetric structure. A significant variation in layer structure was observed in membrane structure upon increase of GO concentration. The channels and voids in the sublayer appear to be more finger-like and lateral upon increase in the GO concentration in membrane matrix. As observed, with GO concentration increased in the prepared membranes, the channels become more significant with increase in porosity. The finger-like pores for GO-PES membranes were wider as compared to pristine PES membranes. These changes in the membrane structure can be attributed to the hydrophilic nature of GO [57]. The addition of GO in the solution casting mixture made it more hydrophilic, which caused a solvent (NMP) and nonsolvent (water) exchange during the phase inversion to yield this wider finger-like channel effect with increased porosity and the lateral structure formation with increasing GO concentration in the prepared membranes [39, 58, 59].

3.3. Wettability and Water Retention Capacity. Table 1 summarizes the results of contact angle measurements and moisture content as water retention of the fabricated membranes. Both parameters provide useful information about the hydrophilicity of that prepared membrane [60]. The contact angle is found to be highest for the M1 pristine PES membrane due to the hydrophobic nature of PES. It would be interesting to discuss the effect of incorporation of GO in the PES membrane to alter the hydrophilicity of the prepared membrane. Contact angles of prepared membranes are presented in Figure 7. As the GO concentration increased in the membrane, the contact angle observed to decrease indicates that the membrane surface became more hydrophilic in accordance to Young and other associated models [60]. During the solvent and nonsolvent exchange in the phase inversion process, GO has more affinity towards the nonsolvent (water). This is attributed to hydrophilic nature of GO. This characteristic of GO tends it to move towards the surface of the membrane during the nonsolvent (water) phase and thus prefers it to be present on the surface of the membrane [61]. The presence of GO on membrane surface causes increased surface hydrophilicity of GO membranes as compared to pristine PES membranes. This explains why the contact angle of the prepared membranes M2–M4 decreased with incorporating GO concentration. However, as the GO incorporation is increased from 0.5 wt. % to 1 wt. %, the contact angle is shown to increase slightly as compared to 0.5%.This observation of decrease of contact angle with increase in GO concentration can be attributed to possible agglomeration of GO due to higher concentration [62]. This effect can lead to decrease in effective surface which subsequently results in reduction of functional groups on the surface to make the membrane more hydrophobic as discussed elsewhere [61].

Water retention shows the maximum moisture content that can be absorbed by a membrane. The results show that the pristine M1 PES membrane had the least water retention capacity that can be attributed to the hydrophobic character of the PES membrane. Membranes with GO concentrations for M2–M4, showed high water retention capacities owing to the hydrophilic nature of GO, to make the membranes relatively more hydrophilic. The hydrophilic GO incorporated

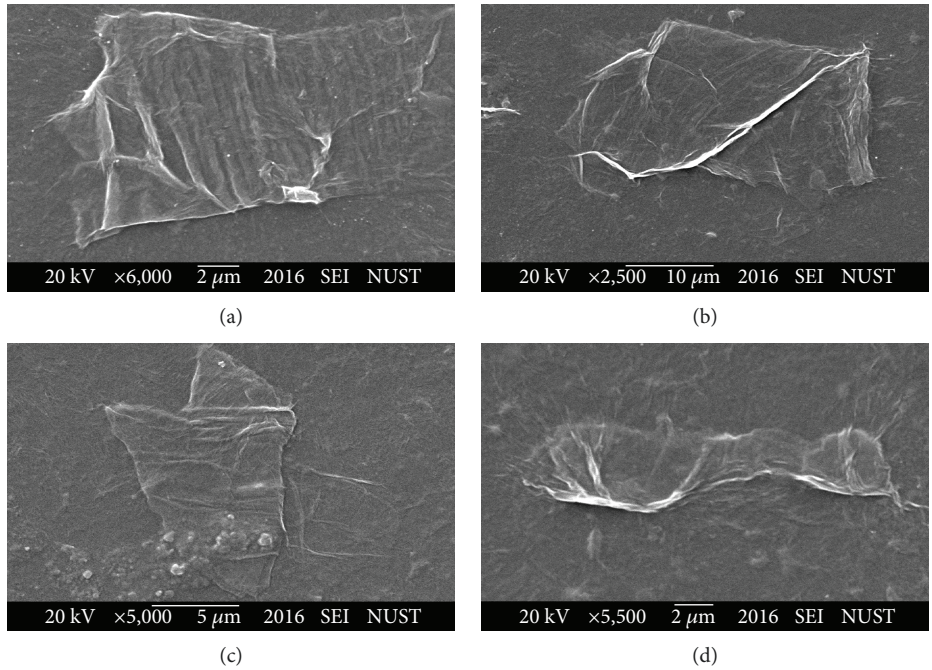

Figure 4: SEM micrographs of the prepared graphene oxide (GO).

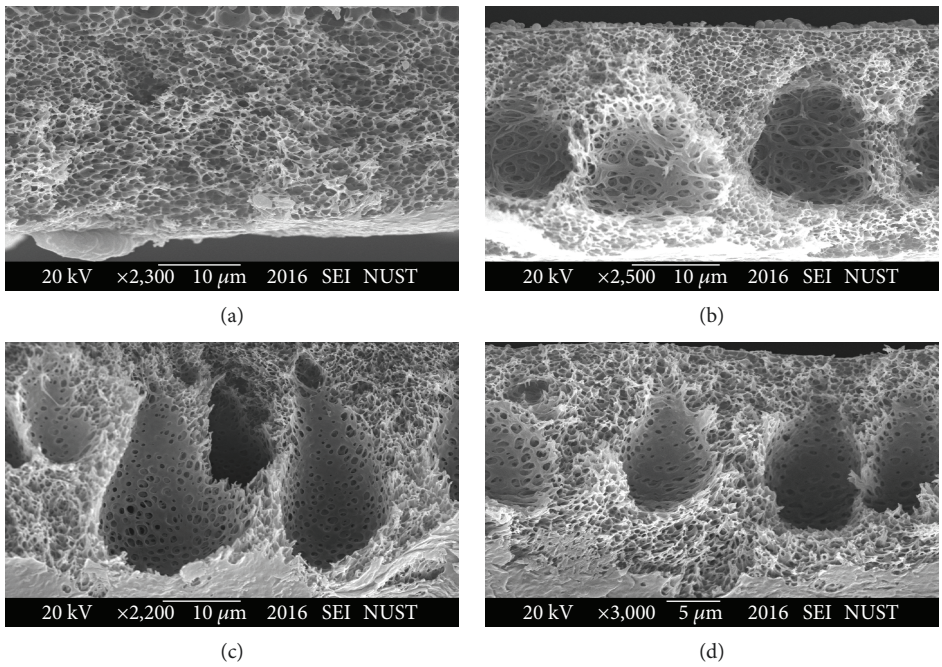

Figure 5: SEM micrographs of fabricated GO-PES membranes showing significant porosity with increasing GO concentration incorporation in the PES matrix membranes: (a) M1 (pristine PES), (b) M2 with 0.25% GO, (c) M3 with 0.5% GO, and (d) M4 with 1.0% GO.

in the membranes causes the retention of water in the membranes [63]. In the case of the M3 membrane with 0.5 wt. % GO, highest water retention was observed. However, there was no significant difference between the water retention capabilities of M3 and M4 membranes. The water retention capacity is observed to decrease as the GO concentration is increased from 0.5 wt. % for the M3 membrane to 1 wt. % for the M4 membrane. A possible explanation for this observation can be again the agglomeration of GO due to higher incorporation. The agglomeration causes decrease in the effective hydrophilicity of the GO as discussed earlier.

3.4. Water Flux. Table 1 shows the flux values calculated for the fabricated membranes at 79.99 KPa. It was observed that in general, increasing the amount of GO in the membrane increased the flux of the prepared membrane. For pristine

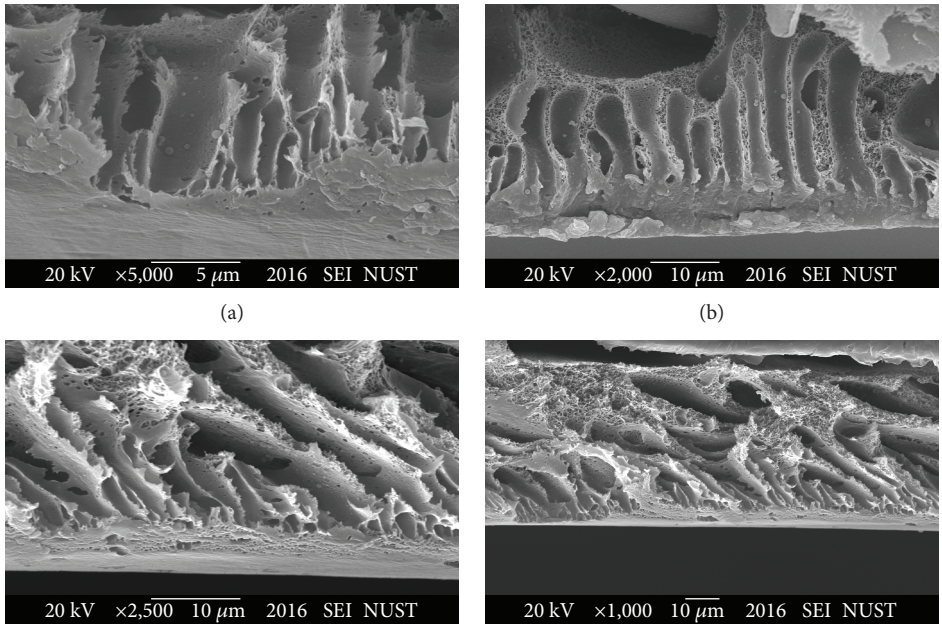

Figure 6: SEM micrographs of the prepared GO-PES membranes: (a) pristine PES membranes, (b) 0.25 wt. % (M1), (c) 0.5 wt. % (M2), and (d) 1.0 wt. % (M4).

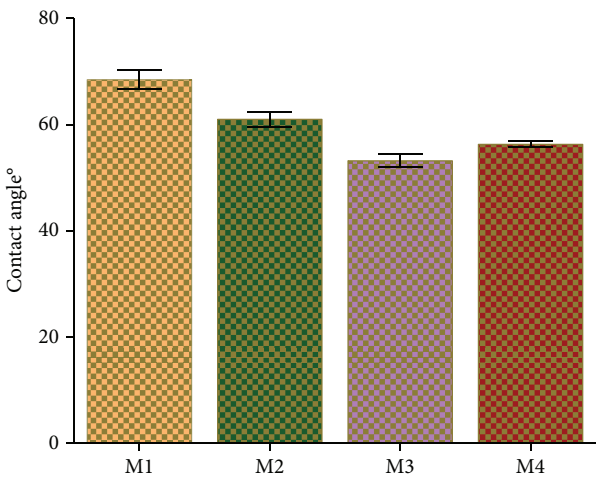

Figure 7: Contact angle values of the prepared membranes. Three measurements for each membrane were taken, and error bar represents standard deviation.

PES membrane M1, the lowest flux value of 28 l/m^2·h was observed, while M3 had the highest flux rate of 142 l/m^2·h. The low flux rate of pristine PES membrane M1 is attributed to the hydrophobic nature of PES as well as the morphological structure of pristine PES membranes with small pores and low pore density as well as intricate finger-like morphological underlying channels.

With the addition of GO as nanofiller in the prepared membranes, however, the flux of the membranes increases significantly as shown in Figure 8. This is explained as a hydrophilic character of GO that makes these membranes relatively more hydrophilic as compared to PES. The observation of higher flux for GO-incorporated membranes can also be explained in relation to their morphological structure and porosity. The formation of relatively wider finger-like channels in GO-incorporated membranes as in the case of M2, M3, and M4 causes increased flux as compared to that of the pristine M1 membrane. The trend observed in flux values is consistent with the contact angles measured for the prepared membranes. A significantly higher flux value (l/m^2·h) was observed for M3 (0.5 wt. % GO) as compared to other GO-incorporated membranes. This can be attributed to the significant lateral orientation of finger-like channels in this membrane [64]. As the GO concentration increases from 0.5% for M3 to 1% for M4, the flux rate decreases. The agglomeration of GO due to its higher incorporation is causing the narrowing of pores to explain the decline in flux rate for this type of membrane. The flux values obtained for the pristine and GO-PES membranes clearly indicated the significance of variable GO concentration incorporated to control as well as optimize the important parameter of water flux.

3.5. Antibacterial Activity of Graphene Oxide and GO-PES Membranes. Graphene oxide showed significant antibacterial activity as illustrated by the results as shown in Figure 9. The antibacterial activity of GO increased with increasing concentration. A P value of <0.0001 was obtained for all the samples containing GO as compared to control. Highest percentage reduction was observed with 500 μg/ml GO (P value < 0.0001). Increase in antibacterial effect with increasing GO concentration was consistent with previous findings [42]. A significant increase in antibacterial activity

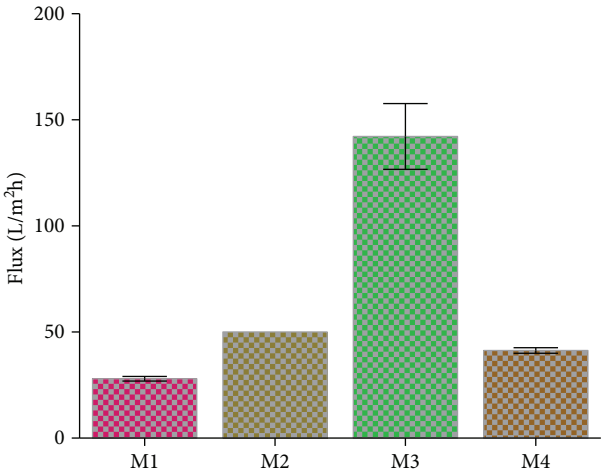

Figure 8: Pure water flux calculated for the fabricated membranes. Error bars represent standard deviation, and three measurements were taken for water flux.

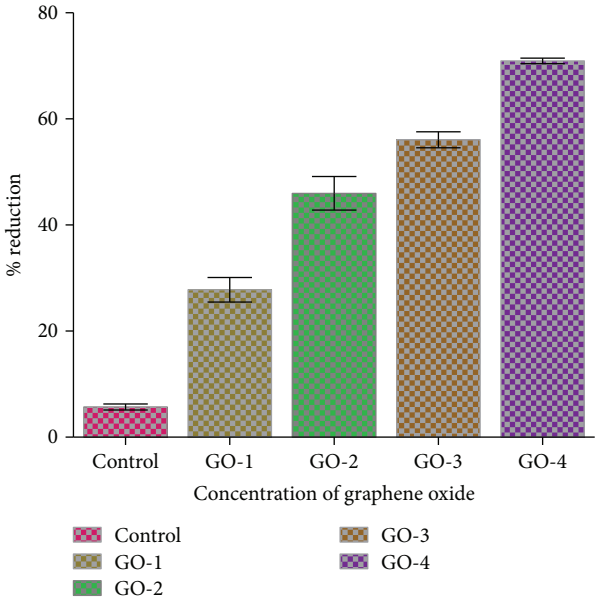

Figure 9: Antibacterial activity of various graphene oxide (GO) concentrations against *S. typhi*.

or percentage reduction was obtained with increase in GO for each sample as evident from Table 1.

Antibacterial activity of GO was tested against *P. syringae* and *X. campestris* that showed a decrease in survival rate of the bacterial cells with increase in GO concentration [33]. In present work, GO shows significant antibacterial activity against *S. typhi* and the antibacterial activity is found to be highly concentration dependent. GO-incorporated PES membranes showed significant antibacterial activity as evident from the results given in Table 1. The antibacterial activity of GO-PES membranes increased with increasing GO concentration in the prepared membrane. Highest percentage reduction was observed with the M4 membrane that was found to be 69.4% as shown in Figure 10.

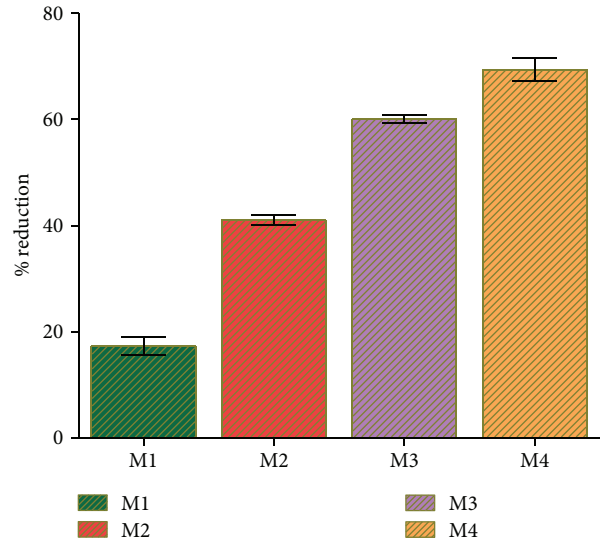

Figure 10: Antibacterial activity of various fabricated membranes against *S. typhi*.

The functional moieties present on GO and the hydrophilicity of GO cause oxidative stress and radical production-induced cell lysis and death of the bacterial cells [34]. The GO present on the surface of the membranes causes bacterial cell death and loss of cell viability [34]. The antibacterial activity of GO can be explained by the fact that the sharp edges of GO penetrate the cell membrane of the bacteria. Additionally, GO also has an oxidative nature which is responsible for bacterial cell membrane disruption. The GO nanosheets cut through the cell membrane and start to extract the phospholipids. As the concentration of GO is increased, consequently, more nanosheets are available to cut and extract phospholipids leading to an increment in the death of bacterial cells [65].

Percentage reduction of *S. typhi* cells by the pristine PES M1 membrane is also observed. This can be explained by entrapment of bacterial cells in membrane pores of the pure PES membrane. GO-incorporated membranes, however, show significantly higher percentage reduction in *S. typhi* cells, with a pattern of high percentage reduction with increasing GO concentration.

Representation of scanning electron microscopy (SEM) images of the prepared M3 membrane is shown in Figure 11, following shake flask method and washing with saline. The presence of live and dead *S. typhi* bacteria on the membrane surface is evident. Intact live bacterial cells (indicated by green arrow signs) can be seen; the glow at the edges of the bacteria is showing that the bacterial membrane is still intact. Dead bacteria (indicated by red arrow signs) can also be seen, with ruptured membranes. Similar observations have been reported previously [29–31, 66].

4. Conclusions

Graphene oxide-PES mixed matrix membranes with variable concentration of GO were prepared for specific antimicrobial activity against *Salmonella typhi* present in water. It was

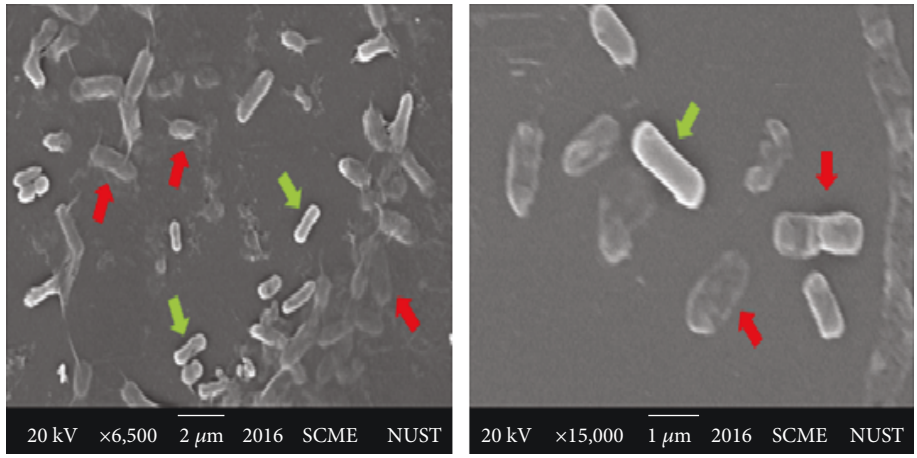

Figure 11: SEM micrographs of the M3 membrane with 0.5 wt. % GO concentration following shake flask method to specifically highlight *S. typhi* bacterial cells.

observed that variable GO concentrations have notable differences in their properties and performance. As GO concentration in the PES membrane increases up to 0.5 wt. %, water retention, wettability, flux, and antibacterial activity were observed to be enhanced. However, further increase in GO concentration incorporation is observed to produce its agglomeration to cause relatively lower water retention, flux, and wettability. Membrane characterization and testing indicated that as compared to the pristine PES membrane, the incorporation of increasing concentration of GO had a significant effect on membrane morphology, wettability, water retaining capacity, and flux. GO-PES membranes with a GO concentration of 0.5% membrane produced significant and optimized results for water retention, pure water flux, and antibacterial activity against typhoid-causing bacterium—*S. typhi*—and can be used in water treatment applications. Thus, keeping the controllable and optimal concentration of GO up to 0.5 wt. %, synergistic effect of GO with other antibacterial fillers can also be investigated. Moreover, a broad spectrum of bacterial species/strains can also be studied using membranes with variable concentrations of GO in the membrane matrix.

Data Availability

The data used to support the findings of this study are available from the corresponding author upon request.

Conflicts of Interest

The authors declare that there is no conflict of interest regarding the publication of this paper.

Acknowledgments

The authors would like to acknowledge the support from SCME and SMME labs to carry out the experimental work. The support from Mr. Shams Din to carry out SEM analysis is highly acknowledged. Dr. Nasir M. Ahmad acknowledges the support from the Higher Education Commission, Pakistan, National Program for Universities (NRPU) project nos. 3526 and 3620 to support the research.

References

[1] C. L. Moe and R. D. Rheingans, "Global challenges in water, sanitation and health," *Journal of Water and Health*, vol. 4, Supplement 1, pp. 41–57, 2006.

[2] World Health Organization and UN-Water, *UN-Water Global Analysis and Assessment of Sanitation and Drinking-Water (GLAAS) 2017 Report*, 2017.

[3] I. A. Shiklomanov, "Appraisal and assessment of world water resources," *Water International*, vol. 25, no. 1, pp. 11–32, 2000.

[4] E. R. Choffnes and A. Mack, Eds., *Medicine, I.o., Global Issues in Water, Sanitation, and Health: Workshop Summary*, The National Academies Press, Washington, DC, USA, 2009.

[5] X. Qu, P. J. J. Alvarez, and Q. Li, "Applications of nanotechnology in water and wastewater treatment," *Water Research*, vol. 47, no. 12, pp. 3931–3946, 2013.

[6] M. A. Montgomery and M. Elimelech, "Water and sanitation in developing countries: including health in the equation," *Environmental Science & Technology*, vol. 41, no. 1, pp. 17–24, 2007.

[7] S. Baldursson and P. Karanis, "Waterborne transmission of protozoan parasites: review of worldwide outbreaks - an update 2004-2010," *Water Research*, vol. 45, no. 20, pp. 6603–6614, 2011.

[8] J. A. Crump and E. D. Mintz, "Global trends in typhoid and paratyphoid fever," *Clinical Infectious Diseases*, vol. 50, no. 2, pp. 241–246, 2010.

[9] M. Antillón, J. L. Warren, F. W. Crawford et al., "The burden of typhoid fever in low- and middle-income countries: a meta-regression approach," *PLoS Neglected Tropical Diseases*, vol. 11, no. 2, article e0005376, 2017.

[10] H. Ma, C. Burger, B. S. Hsiao, and B. Chu, "Ultrafine polysaccharide Nanofibrous membranes for water purification," *Biomacromolecules*, vol. 12, no. 4, pp. 970–976, 2011.

[11] M. Hassan, R. Abou-Zeid, E. Hassan, L. Berglund, Y. Aitomäki, and K. Oksman, "Membranes based on cellulose nanofibers and activated carbon for removal of Escherichia coli bacteria from water," *Polymer*, vol. 9, no. 12, p. 335, 2017.

[12] A. Malekizadeh and P. M. Schenk, "High flux water purification using aluminium hydroxide hydrate gels," *Scientific Reports*, vol. 7, no. 1, article 17437, 2017.

[13] M. M. Pendergast and E. M. V. Hoek, "A review of water treatment membrane nanotechnologies," *Energy & Environmental Science*, vol. 4, no. 6, pp. 1946–1971, 2011.

[14] Y.-F. Guo, P.-C. Sun, and J.-F. Wei, "New insight into the fouling behavior of hydrophobic and hydrophilic polypropylene membranes in integrated membrane bioreactors," *Environmental Technology*, vol. 39, no. 24, pp. 1–10, 2018.

[15] S. S. Madaeni, "The application of membrane technology for water disinfection," *Water Research*, vol. 33, no. 2, pp. 301–308, 1999.

[16] T. Peters, "Membrane technology for water treatment," *Chemical Engineering & Technology*, vol. 33, no. 8, pp. 1233–1240, 2010.

[17] B. Nicolaisen, "Developments in membrane technology for water treatment," *Desalination*, vol. 153, no. 1-3, pp. 355–360, 2003.

[18] T. Nguyen, F. A. Roddick, and L. Fan, "Biofouling of water treatment membranes: a review of the underlying causes, monitoring techniques and control measures," *Membranes*, vol. 2, no. 4, pp. 804–840, 2012.

[19] J. Kim and B. Van der Bruggen, "The use of nanoparticles in polymeric and ceramic membrane structures: review of manufacturing procedures and performance improvement for water treatment," *Environmental Pollution*, vol. 158, no. 7, pp. 2335–2349, 2010.

[20] L. YAN, Y. LI, C. XIANG, and S. XIANDA, "Effect of nano-sized Al_2O_3-particle addition on PVDF ultrafiltration membrane performance," *Journal of Membrane Science*, vol. 276, no. 1-2, pp. 162–167, 2006.

[21] A. Razmjou, J. Mansouri, and V. Chen, "The effects of mechanical and chemical modification of TiO_2 nanoparticles on the surface chemistry, structure and fouling performance of PES ultrafiltration membranes," *Journal of Membrane Science*, vol. 378, no. 1-2, pp. 73–84, 2011.

[22] M. Gholipour-Mahmoudalilou, H. Roghani-Mamaqani, R. Azimi, and A. Abdollahi, "Preparation of hyperbranched poly (amidoamine)-grafted graphene nanolayers as a composite and curing agent for epoxy resin," *Applied Surface Science*, vol. 428, pp. 1061–1069, 2018.

[23] R. W. Baker, "Membrane Technology," in *Kirk-Othmer Encyclopedia of Chemical Technology*, John Wiley & Sons, Inc, 2000, in.

[24] C. Zhao, J. Xue, F. Ran, and S. Sun, "Modification of polyethersulfone membranes – a review of methods," *Progress in Materials Science*, vol. 58, no. 1, pp. 76–150, 2013.

[25] J.-J. Qin, M. H. Oo, and Y. Li, "Development of high flux polyethersulfone hollow fiber ultrafiltration membranes from a low critical solution temperature dope via hypochlorite treatment," *Journal of Membrane Science*, vol. 247, no. 1-2, pp. 137–142, 2005.

[26] B. Van der Bruggen, "Chemical modification of polyethersulfone nanofiltration membranes: a review," *Journal of Applied Polymer Science*, vol. 114, no. 1, pp. 630–642, 2009.

[27] A. Abdollahi, H. Roghani-Mamaqani, M. Salami-Kalajahi, A. Mousavi, B. Razavi, and S. Shahi, "Preparation of organic-inorganic hybrid nanocomposites from chemically modified epoxy and novolac resins and silica-attached carbon nanotubes by sol-gel process: investigation of thermal degradation and stability," *Progress in Organic Coatings*, vol. 117, pp. 154–165, 2018.

[28] A. Abdollahi, H. Roghani-Mamaqani, M. Salami-Kalajahi, B. Razavi, A. Mousavi, and S. Shahi, "Preparation of hybrid composites based on epoxy, novolac, and epoxidized novolac resins and silica nanoparticles with high char residue by sol-gel method," *Polymer Composites*, vol. 38, 2017.

[29] D. I. Gwon, S. S. Lee, and E. Y. Kim, "Cefotaxime-eluting covered self-expandable stents in a canine biliary model: scanning electron microscopic study of biofilm formation," *Acta Radiologica*, vol. 53, no. 10, pp. 1127–1132, 2012.

[30] H. Li, Q. Chen, J. Zhao, and K. Urmila, "Enhancing the antimicrobial activity of natural extraction using the synthetic ultrasmall metal nanoparticles," *Scientific Reports*, vol. 5, no. 1, article 11033, 2015.

[31] A. Tripathy, P. Sen, B. Su, and W. H. Briscoe, "Natural and bioinspired nanostructured bactericidal surfaces," *Advances in Colloid and Interface Science*, vol. 248, pp. 85–104, 2017.

[32] P. Marques, G. Gonçalves, S. Cruz et al., "Functionalized graphene nanocomposites," in *Advances in Nanocomposite Technology, Ch. 11*, A. Hashim, Ed., InTech, Rijeka, 2011.

[33] J. Chen, H. Peng, X. Wang, F. Shao, Z. Yuan, and H. Han, "Graphene oxide exhibits broad-spectrum antimicrobial activity against bacterial phytopathogens and fungal conidia by intertwining and membrane perturbation," *Nanoscale*, vol. 6, no. 3, pp. 1879–1889, 2014.

[34] J. Zhu, J. Wang, J. Hou, Y. Zhang, J. Liu, and B. van der Bruggen, "Graphene-based antimicrobial polymeric membranes: a review," *Journal of Materials Chemistry A*, vol. 5, no. 15, pp. 6776–6793, 2017.

[35] M. Z. Fahmi, M. Wathoniyyah, M. Khasanah, Y. Rahardjo, S. Wafiroh, and A. Abdulloh, "Incorporation of graphene oxide in polyethersulfone mixed matrix membranes to enhance hemodialysis membrane performance," *RSC Advances*, vol. 8, no. 2, pp. 931–937, 2018.

[36] Y. Zhu, S. Murali, W. Cai et al., "Graphene and graphene oxide: synthesis, properties, and applications," *Advanced Materials*, vol. 22, no. 35, pp. 3906–3924, 2010.

[37] L. Jin, Z. Wang, S. Zheng, and B. Mi, "Polyamide-crosslinked graphene oxide membrane for forward osmosis," *Journal of Membrane Science*, vol. 545, pp. 11–18, 2018.

[38] A. Mousavi, H. Roghani-Mamaqani, M. Salami-Kalajahi, S. Shahi, and A. Abdollahi, "Grafting of silica nanoparticles at the surface of graphene for application in novolac-type phenolic resin hybrid composites," *Materials Chemistry and Physics*, vol. 216, pp. 468–475, 2018.

[39] S. Zinadini, V. Vatanpour, A. A. Zinatizadeh, M. Rahimi, Z. Rahimi, and M. Kian, "Preparation and characterization of antifouling graphene oxide/polyethersulfone ultrafiltration membrane: application in MBR for dairy wastewater treatment," *Journal of Water Process Engineering*, vol. 7, pp. 280–294, 2015.

[40] L. Chen, J. H. Moon, X. Ma et al., "High performance graphene oxide nanofiltration membrane prepared by electrospraying for wastewater purification," *Carbon*, vol. 130, pp. 487–494, 2018.

[41] L. Yu, Y. Zhang, B. Zhang, J. Liu, H. Zhang, and C. Song, "Preparation and characterization of HPEI-GO/PES ultrafiltration membrane with antifouling and antibacterial properties," *Journal of Membrane Science*, vol. 447, pp. 452–462, 2013.

[42] Y. Gao, J. Wu, X. Ren et al., "Impact of graphene oxide on the antibacterial activity of antibiotics against bacteria," *Environmental Science: Nano*, vol. 4, no. 5, pp. 1016–1024, 2017.

[43] A. D. Pithie and M. J. Wood, "Treatment of typhoid fever and infectious diarrhoea with ciprofloxacin," *The Journal of Antimicrobial Chemotherapy*, vol. 26, Supplement F, pp. 47–53, 1990.

[44] P. Rupali, O. C. Abraham, M. V. Jesudason et al., "Treatment failure in typhoid fever with ciprofloxacin susceptible *Salmonella enterica* serotype typhi," *Diagnostic Microbiology and Infectious Disease*, vol. 49, no. 1, pp. 1–3, 2004.

[45] C. Dolecek, T. T. Phi la, N. N. Rang et al., "A multi-center randomised controlled trial of gatifloxacin versus azithromycin for the treatment of uncomplicated typhoid fever in children and adults in Vietnam," *PLoS One*, vol. 3, no. 5, article e2188, 2008.

[46] M. R. Capoor, D. Rawat, D. Nair et al., "*In vitro* activity of azithromycin, newer quinolones and cephalosporins in ciprofloxacin-resistant *Salmonella* causing enteric fever," *Journal of Medical Microbiology*, vol. 56, no. 11, pp. 1490–1494, 2007.

[47] T. Kadhiravan, N. Wig, A. Kapil, S. K. Kabra, K. Renuka, and A. Misra, "Clinical outcomes in typhoid fever: adverse impact of infection with nalidixic acid-resistant *Salmonella typhi*," *BMC Infectious Diseases*, vol. 5, no. 1, p. 37, 2005.

[48] A. Singh, G. Sinsinbar, M. Choudhary et al., "Graphene oxide-chitosan nanocomposite based electrochemical DNA biosensor for detection of typhoid," *Sensors and Actuators B: Chemical*, vol. 185, pp. 675–684, 2013.

[49] N. M. Huang, H. N. Lim, C. H. Chia, M. A. Yarmo, and M. R. Muhamad, "Simple room-temperature preparation of high-yield large-area graphene oxide," *International Journal of Nanomedicine*, vol. 6, pp. 3443–3448, 2011.

[50] I. Munnawar, S. S. Iqbal, M. N. Anwar et al., "Synergistic effect of chitosan-zinc oxide hybrid nanoparticles on antibiofouling and water disinfection of mixed matrix polyethersulfone nanocomposite membranes," *Carbohydrate Polymers*, vol. 175, pp. 661–670, 2017.

[51] E. Saljoughi, M. Sadrzadeh, and T. Mohammadi, "Effect of preparation variables on morphology and pure water permeation flux through asymmetric cellulose acetate membranes," *Journal of Membrane Science*, vol. 326, no. 2, pp. 627–634, 2009.

[52] R. Hazan, Y. A. Que, D. Maura, and L. G. Rahme, "A method for high throughput determination of viable bacteria cell counts in 96-well plates," *BMC Microbiology*, vol. 12, no. 1, pp. 259–259, 2012.

[53] T. F. Emiru and D. W. Ayele, "Controlled synthesis, characterization and reduction of graphene oxide: a convenient method for large scale production," *Egyptian Journal of Basic and Applied Sciences*, vol. 4, no. 1, pp. 74–79, 2017.

[54] M. Naebe, J. Wang, A. Amini et al., "Mechanical property and structure of covalent functionalised graphene/epoxy nanocomposites," *Scientific Reports*, vol. 4, no. 1, article 4375, 2015.

[55] S. M. Badawy, "Synthesis of high-quality graphene oxide from spent mobile phone batteries," *Environmental Progress & Sustainable Energy*, vol. 35, no. 5, pp. 1485–1491, 2016.

[56] Y. Jiang, P. Biswas, and J. D. Fortner, "A review of recent developments in graphene-enabled membranes for water treatment," *Environmental Science: Water Research & Technology*, vol. 2, no. 6, pp. 915–922, 2016.

[57] Q. Liu, L. Li, X. Jin, C. Wang, and T. Wang, "Influence of graphene oxide sheets on the pore structure and filtration performance of a novel graphene oxide/silica/polyacrylonitrile mixed matrix membrane," *Journal of Materials Science*, vol. 53, no. 9, pp. 6505–6518, 2018.

[58] B. M. Ganesh, A. M. Isloor, and A. F. Ismail, "Enhanced hydrophilicity and salt rejection study of graphene oxide-polysulfone mixed matrix membrane," *Desalination*, vol. 313, pp. 199–207, 2013.

[59] J. Lee, H. R. Chae, Y. J. Won et al., "Graphene oxide nanoplatelets composite membrane with hydrophilic and antifouling properties for wastewater treatment," *Journal of Membrane Science*, vol. 448, pp. 223–230, 2013.

[60] Y. Yuan and T. R. Lee, "Contact angle and wetting properties," in *Surface Science Techniques*, G. Bracco and B. Holst, Eds., pp. 3–34, Springer Berlin Heidelberg, Berlin, Heidelberg, 2013.

[61] A. K. Shukla, J. Alam, M. Alhoshan, L. A. Dass, and M. R. Muthumareeswaran, "Development of a nanocomposite ultrafiltration membrane based on polyphenylsulfone blended with graphene oxide," *Scientific Reports*, vol. 7, no. 1, article 41976, 2017.

[62] Z. Li, J. Chu, C. Yang et al., "Effect of functional groups on the agglomeration of graphene in nanocomposites," *Composites Science and Technology*, vol. 163, pp. 116–122, 2018.

[63] S. Zheng, Q. Tu, J. J. Urban, S. Li, and B. Mi, "Swelling of graphene oxide membranes in aqueous solution: characterization of interlayer spacing and insight into water transport mechanisms," *ACS Nano*, vol. 11, no. 6, pp. 6440–6450, 2017.

[64] D. Qin, Z. Liu, D. Delai Sun, X. Song, and H. Bai, "A new nanocomposite forward osmosis membrane custom-designed for treating shale gas wastewater," *Scientific Reports*, vol. 5, no. 1, article 14530, 2015.

[65] Y. Tu, M. Lv, P. Xiu et al., "Destructive extraction of phospholipids from *Escherichia coli* membranes by graphene nanosheets," *Nature Nanotechnology*, vol. 8, no. 8, pp. 594–601, 2013.

[66] F. Perreault, A. F. de Faria, S. Nejati, and M. Elimelech, "Antimicrobial properties of graphene oxide nanosheets: why size matters," *ACS Nano*, vol. 9, no. 7, pp. 7226–7236, 2015.